Pakistan Veterinary Journal

ISSN: 0253-8318 (PRINT), 2074-7764 (ONLINE)
DOI: 10.29261/pakvetj/2024.255

RESEARCH ARTICLE

Protective Effects of SHLO on LPS-Induced Lung Injury via TLR4/Myd88-ERK Signaling Pathway and Intestinal Flora Regulation

Yujie Han[1,2,3], Zongshu Zhang[1], Heyun Yang[1,2], Na Zhang[1,2], Cui Lin[1,2], Ali Raza[4], Ahmed Ezzat Ahmed[5], Layla A. Almutairi[6], Amir Iftikhar Malik[4], Sammina Mahmood[7], Qinghui Jia[3*] and Xinghua Zhao[1,2*]

[1]College of Traditional Chinese Veterinary Medicine of Hebei Agricultural University, Baoding, 071000, PR China.
[2]Hebei Province Traditional Chinese Veterinary Medicine Technology Innovation Center, Baoding, 071000, PR China.
[4]Faculty of Veterinary and Animal Sciences, The Islamia University Bahawalpur 63100, Pakistan
[5]Department of Biology, College of Science, King Khalid University, Abha 61413, Saudi Arabia
[6]Department of Biology, College of Science Princess Nourah bint Abdulrahman University, P.O. Box 84428, Riyadh 11671, Saudi Arabia
[7]Department of Botany, Division of Science and Technology, University of Education, Lahore. Pakistan
*Corresponding author: xianzhaoxinghua@163.com

ARTICLE HISTORY (24-492)

Received: August 15, 2024
Revised: September 22, 2024
Accepted: September 24, 2024
Published online: September 27, 2024

Key words:
Shuanghuanglian
Volatile oil
LPS
pulmonary inflammation
TLR4
Myd88
ERK

ABSTRACT

The "Shuanghuanglian" formula, simplified from the classic formula "Yin Qiao San", is composed of the Honeysuckle flower, *Scutellaria* root and *Forsythia* fruit. Its primary effects include dispelling wind, relieving exterior syndrome, and clearing heat and toxic materials. The traditional "Shuanghuanglian" (SHL) preparation method requires prolonged heating that results in the loss of volatile oil components and diminishes its efficacy. This study centered on developing an enhanced "Shuanghuanglian" volatile oil-infused soluble powder (SHLO) and evaluating its therapeutic efficacy and mechanisms using a mouse pneumonia model. Our findings demonstrate that SHLO administration significantly restores lung tissue damage and mitigates LPS-induced pulmonary inflammation. SHLO intervention led to a notable reduction in TUNEL-positive lung cells and levels of IL-6 ($P<0.01$), IL-1β ($P<0.001$), and TNF-α ($P<0.05$) in bronchoalveolar lavage fluid (BALF) triggered by LPS. Furthermore, SHLO markedly suppressed p-ERK levels without substantially influencing p-JNK levels or p-NF-κB p65 levels. The relative traces of p-ERK, MyD88, and TLR4 in lung tissues were notably decreased in the SHLO group relative to the LPS group. Additionally, SHLO reduced the proportion of an unclassified *Muribaculaceae* genus while increasing *Akkermansia* levels in the gut microbiota. In summary, SHLO effectively defends against LPS-induced lung damage through the inhibition of the TLR4/MyD88 and p-ERK signaling pathways and modulating gut microbiota.

To Cite This Article: Han Y, Zhang Z, Yang H, Zhang N, Lin C, Raza A, Ahmed AE, Almutairi LA, Malik AI, Mahmood S, Jia Q and Zhao X, 2024. Protective effects of shlo on lps-induced lung injury via tlr4/myd88-erk signaling pathway and intestinal flora regulation. Pak Vet J, 44(3): 776-784. http://dx.doi.org/10.29261/pakvetj/2024.255

INTRODUCTION

Pneumonia is an inflammation of the lungs that affects the peripheral airway, alveoli, and pulmonary interstitium. Acute bacterial lung infections trigger strong inflammatory responses, but excessive inflammatory response can lead to lung injury, and secondary infection and further aggravate the pneumonia (Deshpande and Zou, 2020; Arbaga *et al.*, 2023). Clinically, antibiotics and anti-infective drugs are typically used to combat the bacteria. However, the phenomenon of antibiotic resistance has significantly reduced the clinical efficacy of antibiotic treatment for pneumonia (Botelho *et al.*, 2019; Pang *et al.*, 2019). Traditional Chinese medicine offers alternative treatments for lung diseases by inhibiting pathogens, regulating the immune system, and offering the advantages of multi-target effects with a low risk of drug resistance (Ma *et al.*, 2019; Akpinar *et al.*, 2023). The "Shuanghuanglian" (SHL) formula, simplified from the "Yin Qiao San" formula documented in Item Differentiation of Warm Febrile Diseases (Ma *et al.*, 2021), published in the Qing Dynasty in China, includes Honeysuckle flower (*Lonicera japonica)*, *Scutellaria* root (*Scutellaria baicalensis)* and *Forsythia* fruit (*Forsythia*

suspensa). The primary effects of the SHL formula include dispelling wind, relieving exterior syndrome, and clearing heat and toxins (Li *et al.,* 2023). Various SHL-derived medicines, including Shuanghuanglian oral liquid, granules, injections, and capsules, have been approved by CFDA and are included in the Clinical Medication Guidelines of the People's Republic of China Pharmacopoeia (Chinese Pharmacopoeia Commission, 2017).

Chinese herbal medicine is increasingly being used to maintain human and animal health, prevent or treat diseases due to its low toxicity, few side effects, and low cost. Traditional Chinese herbal medicine is mostly used in the form of monomers or combinations of compound formulas to reduce side effects or enhance therapeutic effects (Shi *et al.,* 2019; Men *et al.,* 2022). Recent studies have shown that SHL oral liquid can reduce inflammatory cell infiltration, inhibit virus replication, alleviate lung injury, and exhibit significant antiviral effects against influenza viruses (H1N1, H5N1), respiratory syncytial virus, and rotavirus (Wu *et al*., 2005; Liu *et al*., 2015; Tang *et al*., 2018; Yi, 2018). Currently, SHL oral liquid is commonly administered in the clinical management of influenza and pneumonia in poultry and livestock (Tang *et al.*, 2018). While not explicitly recommended for COVID-19 pneumonia, data mining of TCM treatments for COVID-19 frequently highlights the use of Honeysuckle flower, *Scutellaria* root, and *Forsythia* fruit (Xi *et al.*, 2020; Ding *et al.,* 2022). Lipopolysaccharide (LPS) is a primary element of the cell wall in Gram-negative bacteria, which is capable of stimulating inflammatory cells, especially alveolar macrophages in the trachea leading to the elicitation of pathogenic mediators, followed by neutrophil recruitment**,** and injured tissue (Vemula *et al.,* 2024). Therefore, intratracheal instillation of LPS was adopted to prepare a mouse pneumonia model in this study. SHL, a composite formulation of traditional Chinese medicine, secures its antipyretic and anti-inflammatory effects via a synergistic interplay across multiple targets and pathways (Ma *et al.,* 2021). However, identifying its effective components and mechanisms of action remains a crucial challenge. Additionally, traditional SHL preparation involves prolonged heating, leading to loss of the volatile oil components and reduced efficacy. This study aimed to develop an improved SHL oral liquid containing volatile oil and investigate its efficacy and underlying mechanisms by using a mouse pneumonia model.

MATERIALS AND METHODS

Materials: Honeysuckle flower, Scutellaria root, and Forsythia fruit were procured from China in July 2023 from Huijutang Pharmaceutical Co. Ltd. ZSGB-BIO Co. Ltd. in Beijing, China, provided the blocking fluid, anti-fluorescence quenching blocker (containing DAPI), TritonX-100 and goat anti-rabbit IgG. Wuhan Boster Bio-Tech Co. Ltd. provided IL-6, IL-10, and IL-1β ELISA kits and primary antibodies for NF-κB p65 (A00284-1), p-ERK1/2 (BM3950), ERK1/2 (BM4326), GADPH (A00227-1), P38MAPK (A00176-2), p-NF-κB p65 (AF2006, Affinity, 65kDa) and p-P38 MAPK (AF4001, Affinity, 43kDa). Sigma (St. Louis, MO, USA) provided the LPS and MTT. TRIzol regent, reverse transcription reagent, and SYBR qPCR Super Mix were procured from Novoprotein Scientific. The remaining reagents, substances**,** and chemicals were designated as scientific grade.

Preparation of SHLO: *Scutellaria* root (750g), and *Forsythia* fruit (1500g) were weighed and soaked in water for 1 hour, then extracted with water three 3 times. The extracts were merged, strained, and concentrated to a density of 1.06-1.08g/ml at 25℃. The concentrate was spray-dried to obtain SHL powder. The same amount of Chinese herb-drug was used for further processing. Volatile oil was collected by heating and distilling, then wrapped with beta-ring paste, dried, and crushed for later use. SHLO was prepared by mixing sucrose, wrapped volatile oil and SHL powder and the Waters 2695 system generated the HPLC chromatogram.

Laboratory animal trial: Five-week-old ICR female mice were purchased from the Biological Institute of China (Beijing Sibeifu Biotechnology Co. Beijing, China). Before the trial, the mice were allowed to acclimate for one week. All animal studies were executed as per the criteria of Laboratory Animal Welfare and received approval (No. HBCT2022161) from the Local Ethics Committee at Hebei Agricultural University, China.

The mice were placed into six groups, each with five individuals: the control, the model, the positive, and the high dose (2.0g/kg), medium (1.5g/kg), and low (0.5g/kg) of SHLO groups. On the first day, the mice in the SHLO groups and the positive group were given corresponding concentrations of SHLO or SHL oral solution while Saline was given orally to the mice in the model group and control group once daily. On the 7th day, LPS solution was administered to the mice, except for those in the control group, via intratracheal instillation with the aid of an endoscope (Ehrentraut *et al.,* 2019). On the 7th day, PBS was introduced into the mice of the control group via intratracheal instillation. Subsequent samples were collected 12 hours after the LPS administration.

Physiological indices and samples collected: Ten hours after the LPS challenge, we anesthetized the mice and collected blood samples to isolate the serum. Bronchoalveolar lavage fluid (BALF), lung tissue, and other samples were collected after euthanizing the mice.

Cell analysis in BALF: 12 hours after tracheal drip LPS, the mice were euthanized, and the neck organs were isolated. The lungs were injected with cold saline and then re-infused with 0.3mL each time after suctioning out four times. The fluid was then pumped back to 1.0mL, the BALF was collected. The BALF was spined in centrifuge machine at 1500 r/min for 10 minutes at 4℃, and precipitate of the cell was resuspended in 50 μl of sterile PBS (Verjans *et al.,* 2018). The total cell number was determined using a cell counter. The resuspended BALF cells were prepared for smear preparation to observe and count neutrophils and giant cells. The smears were stained with the Rachel-Msa Compound Staining Kit.

H&E staining of the lung: Four percent of the para-formaldehyde solution was used to preserve the lung tissue. After some time, various steps were performed including washing, dehydration, hyalinization, embedding, and cutting into 5 μm thick sections according to previous research for H&E staining (Sun *et al.,* 2024).

Immunofluorescence of TLR4 and Myd88 in lung tissues: The sections of lung tissue were treated with 0.02M PBS. The detailed method for immunofluorescence labeling was executed based on a prior investigation by He *et al.* (2023).

Real-time quantitative PCR (RT-qPCR): The lung tissue was lysed using the TRIzol reagent and the total RNA was extracted using the chloroform extraction and isopropanol precipitation method. Reverse transcription was then performed as previously described (Vemula *et al.,* 2024). Gentler 32R PCR apparatus is used to execute Quantitative PCR (qPCR) with FastStart Universal SYBR Green Master Mix. The primer sequences are listed in Table 1. The amplification efficiency and specificity of each primer were validated, while GAPDH was employed as an internal reference gene.

Western blotting: Lysis of lung tissue was performed by using RIPA buffer (phosphatase and protease inhibitors). After centrifugation, the supernatant was collected, and the BCA method was used to assess protein content. Subsequently, protein (30μg) was mixed with 5× Loading Buffer and denatured. The 12% SDS polyacrylamide gels were used to load the denatured samples and protein separation was performed by electrophoresis at 200 V for 45 min. After that, the proteins were run for 90 minutes at 300mA on 0.45μm PVDF membranes. Following the transfer, the membranes were placed for one hour in 5% non-fat milk to block them. After treating them with the primary antibody for a whole night at 4°C, the secondary antibody was incubated. Following three washes with TBST, the Tanon 5200 scanner was used to detect the signals using ECL (Tanon, China).

Enzyme-linked immunosorbent assay (ELISA): IL-6, TNF α and IL-1β levels were measured by ELISA method in the BALF supernatants. Briefly, 100μl of diluted serum sample or the wells were filled with antibody standards and incubated for 90 minutes at 37°C. Subsequently, 100 μl of diluted biotinylated-antibody was inserted and placed for 60 minutes at 37°C. The color development reaction was initiated and stopped after a specific time (Voiriot *et al.,* 2022). At 450 nanometer absorbance, a microplate reader was used for absorbance values, and contention was calculated based on the standard curve.

Gut microbiota analysis: 12 hours after LPS intervention, cecal contents were collected, and total DNA was extracted. The 16S (rRNA) gene subunits having V4 region were amplified to generate 250-nucleotide (nt) Illumina sequencing reads. Sequencing data of the amplified 16S rRNA gene fragments were sorted and assigned using version 1.8 of the QIIME pipeline. Non-metric multidimensional scaling was employed to analyze microbial communities at the genus and species levels (Shin *et al.,* 2022). A comprehensive examination of the microorganism community bar graphs and clustering tree analysis was conducted to assess the impact of SHLO on intestinal microbial communities.

Statistical analysis: The data were expressed as mean ± standard deviation (SD). Statistical significance was determined using ANOVA and Student's t-tests with GraphPad Prism 8.0 software. P-values below 0.05 were deemed statistically significant (White *et al.,* 2022).

RESULTS

HPLC chromatogram of SHLO: About 10 mL of methanol and 5 mg of SHLO were combined to create a 0.5 mg/mL solution. The column was a Diamond C18 column (250 mm × 2.0 mm, 4.5 μm). Methanol (B) and 0.2% phosphoric acid (A) made up the mobile phases. The linear gradient extraction procedure with methanol was as follows: 0–10 min, 17%→30%, 10.1–25 min, 30%→35%, 25.1–35 min, 35%→40%, 35.1–55 min, 40%→60%, 55.1–60 min,60%, 60.1-75 min, 60%→80%, 75.1-110 min, 80%, 110.1-11 min, 80%→17%, 111.1-115 min, 17%. The column temperature was kept at 30 ℃ and 1.0 mL per minute was the flow rate. The HPLC chromatogram of SHLO is shown in Fig. 1. Peak 1, 2, 3, 4, 5, 6, 7, 8, 9, 10, 11, 12, 13, 14, 15 in Fig 1A and B were assigned to neochlorogenic acid, chlorogenic acid, cryptochlorogenic acid, forsythoside I, forsythoside B, forsythoside H, forsythoside A, rutin, phillyrin, baicalin, luteolin, baicalein, 4-Terpineol, β-pinene, and α-pinene, respectively. These compounds may be used as quality markers for SHLO.

Effects of SHLO on the number of total cells, neutrophils, and macrophages in BALF: In the BALF of the SHLO medium and high dosage groups, there were substantially fewer total cells, neutrophils, and macrophages than in the model group ($P<0.01$). Additionally, the number of macrophages neutrophils, and total cells in BALF of the SHLO medium and there was a significant difference ($P<0.01$) between the high-dose groups and the SHL group (Fig. 2)

Histopathological observation

As presented in Fig. 3A, the lungs in the LPS group exhibited consolidation of air spaces and some haemorrhagic areas, indicating significant lung injury. This injury was markedly alleviated by SHLO treatment. Additionally, the LPS group (Fig. 3B) exhibited a considerable increase in TUNEL-positive cells in comparison with the Control group, suggesting increased apoptosis. Treatment with both SHL and SHLO considerably lowered the quantity of TUNEL-positive cells. These findings suggested that SHLO has the potential to inhibit the apoptosis in lungs induced by LPS.

Effects of SHLO on inflammatory cytokine in pneumonia mice induced by LPS: Fig. 4 illustrates that the LPS group had considerably greater levels of IL-1β, IL-6, and TNF-α, than the Control group ($P<0.05$, $P<0.01$). Furthermore, BALF of the SHLO group had substantially lower concentrations of TNF-α, IL-6, and IL-1β than the LPS group ($P<0.05$, $P<0.01$, or $P<0.001$). When compared to the Control group, the mRNA expression levels of TNF α, IL-1β, and IL-6 in the LPS

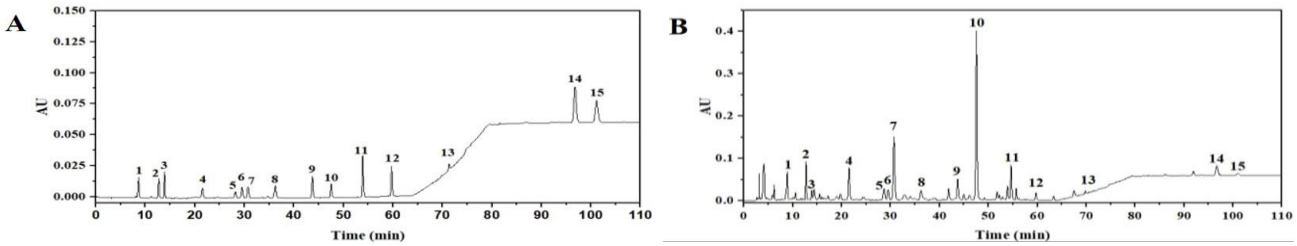

Fig. 1: HPLC chromatogram of SHLO.

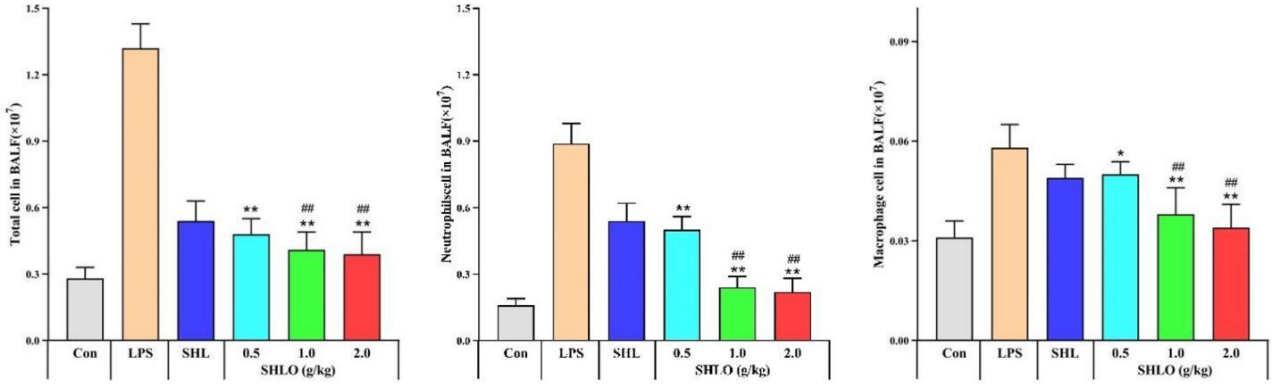

Fig. 2: Effects of LPS, SHL, and SHLO on the number of total cells, neutrophils, macrophages in BALF. **P*<0.05; ***P*<0.01 between LPS and various concentrations of SHLO. ##*P*<0.05 between various concentrations of SHLO. Data are described as the mean ± SEM.

group were considerably higher (P<0.05). Moreover, SHLO down-regulated the production of TNFα, IL-6, and IL-1β in lung tissue.

SHLO regulates the protein expression of the ERK pathway: To investigate the process of action of SHLO, the expression of NF-κB p65, ERK, JNK, p-NF-κB p65, p-ERK, and p-JNK was evaluated in lung tissues by western blotting. SHLO did not influence on the expression of p-JNK, but it dramatically reduced the expression of p-NF-κB p65 and p-ERK (Fig. 5). These findings suggested that the mode of action of SHLO may relate to its influence on the expression of p-ERK.

Immunofluorescence of TLR4, Myd88, and p-ERK: Additionally, the expressions of p-ERK, Myd88 and TLR4 in lung tissue was assessed using immunofluorescence (Fig. 6). The findings demonstrated that the fluorescence intensity of p-ERK, Myd88 and TLR4 in the LPS group was notably stronger compared to the control group. Moreover, p-ERK, Myd88, and TLR4 fluorescence intensity in the SHLO group was considerably less (in comparison to) the LPS group.

SHLO recovers the microbial community composition: Fifteen samples from each group (Control, LPS, and SHLO) were selected to analyze the species composition. There were 806 unique OTUs in the control group, 1033 in the LPS model group, and 728 in the SHLO group (Fig. 7). The results indicated that there was no significant difference in *Lactobacillus* species abundance among the group. However, in contrast to control group, the relative abundance of *Muribaculaceae*_unclassified was significantly increased in the LPS model group (P<0.01), while *Ackermansia* spp. Significant decrease (P<0.01). Following SHLO intervention, the relative abundance of *Muribaculaceae*_unclassified significantly decreased (P<0.01), whereas *Ackermannia* spp. was significantly increased (P<0.01). These findings suggest that SHLO may mitigate intestinal flora alternation induced by LPS-induced acute pneumonia.

DISCUSSION

Pneumonia, which commonly affects elders and children, poses a significant burden on worldwide health (Quinton *et al*., 2018). During the COVID-19 pandemic, traditional herbal treatments have gained increased attention for their demonstrated safety and effectiveness in clinical practice, as well as their accessibility and comprehensive regulatory advantage (Gajewski *et al.*, 2021; Lee *et al.*, 2021). Researchers believe that cytokine release syndrome (CRS) is a primary pathogenic mechanism of COVID-19 (Merad and Martin, 2020; Wang *et al.*, 2020). CRS triggers rapid production of inflammatory cytokines that target inflammatory cytokines sites such as monocytes and neutrophils, effectively damaging bacteria but also resulting in severe injury to normal tissues and organs. Gram-negative bacteria cell walls contain LPS as a major component. LPS infection initiates an inflammatory cascade mediated by inflammatory mediators that is closely linked (Tsikis *et al.*, 2022). Thus, acute respiratory distress syndrome (ARDS) and acute lung injury (ALI) development begins with their onset. Endotracheal LPS stimulation rapidly activates inflammatory cells, particularly alveolar macrophages, triggering the discharge of mediators that cause inflammation and the consequent gathering of neutrophils, tissue damage, pulmonary oedema, and an increase in the response of inflammation (Li *et al.*, 2020). Therefore, an in vivo mouse model of pulmonary inflammation was established via intratracheal LPS instillation, which damages lung epithelium and micro vascular endothelial cells and causes a large influx of

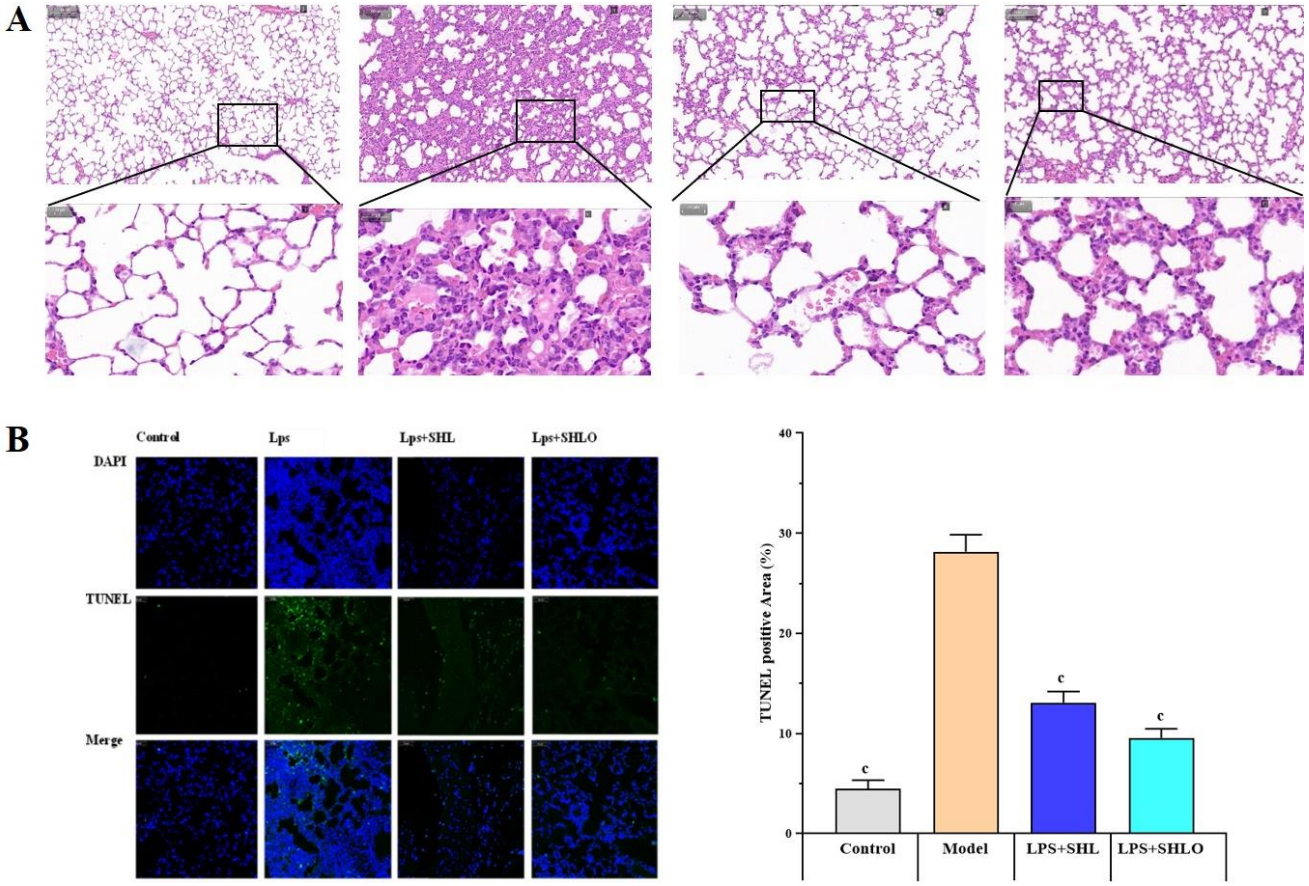

Fig. 3: Effects of LPS, SHL, and SHLO on the lung tissue. (A) The lungs in the LPS group exhibited consolidation of air spaces, some haemorrhagic areas and lung injury compared with SHL and SHLO. (B) TUNEL-positive cells LPS group compare with Control group, suggesting increased apoptosis, while SHLO inhibiting apoptosis rates than SHL. Data are described as the mean ± SEM.

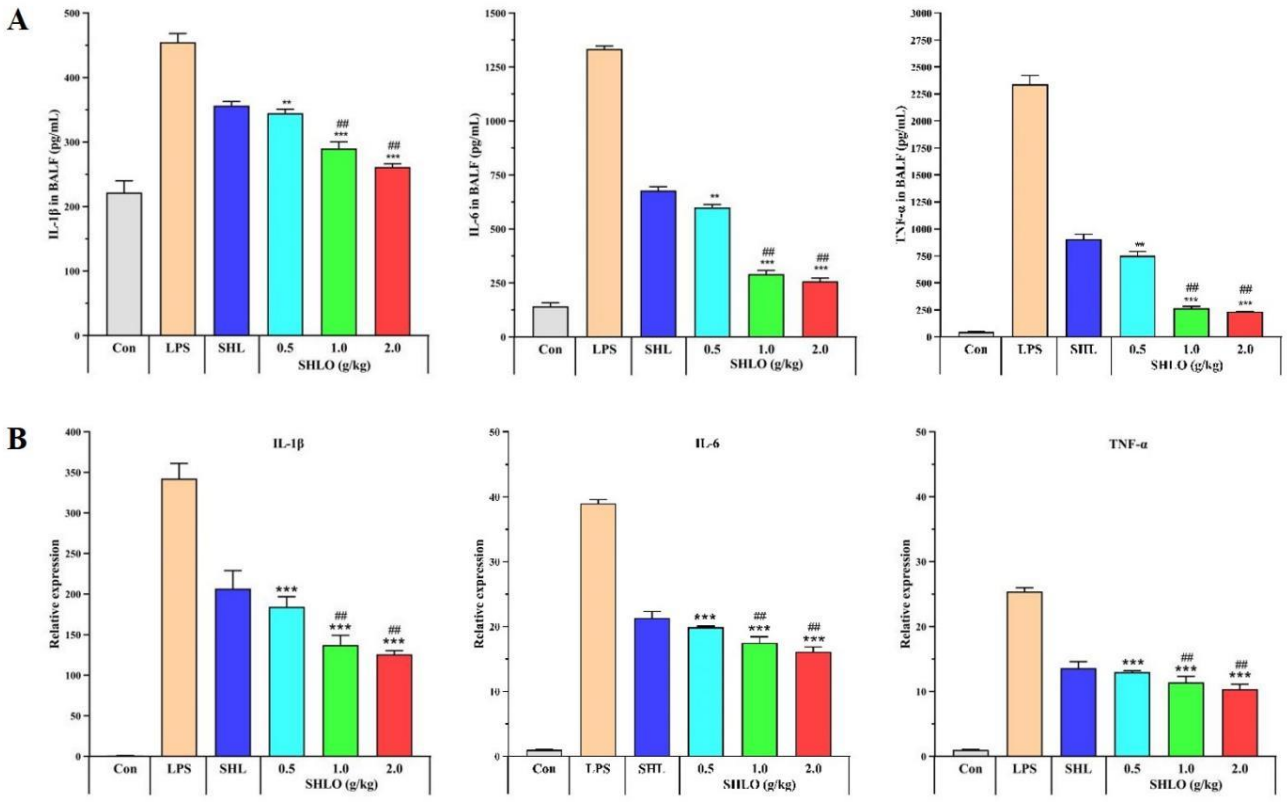

Fig. 4: Effects of SHL and various concentration of SHLO on inflammatory cytokine in pneumonia mice induced by LPS. **P<0.01; ***P<0. 001 between LPS and various concentrations of SHLO. ##P<0.05 between various concentrations of SHLO. Data are described as the mean ± SEM.

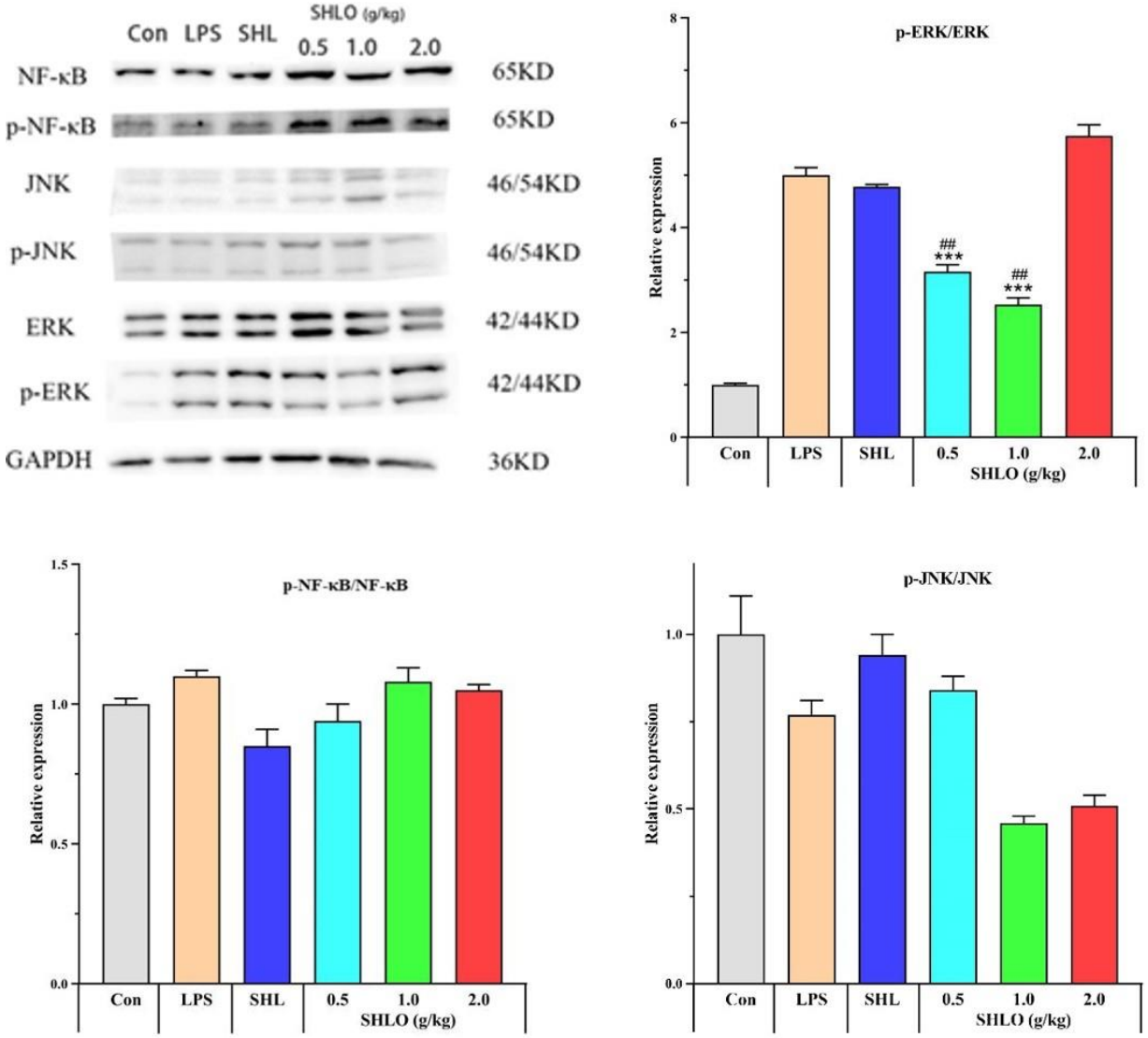

Fig. 5: Effects of SHL and various concentration of regulating the protein expression of ERK pathway**.** ***P<0.001 between LPS and various concentrations of SHLO. ##P<0.05 between various concentrations of SHLO. Data are described as the mean ± SEM.

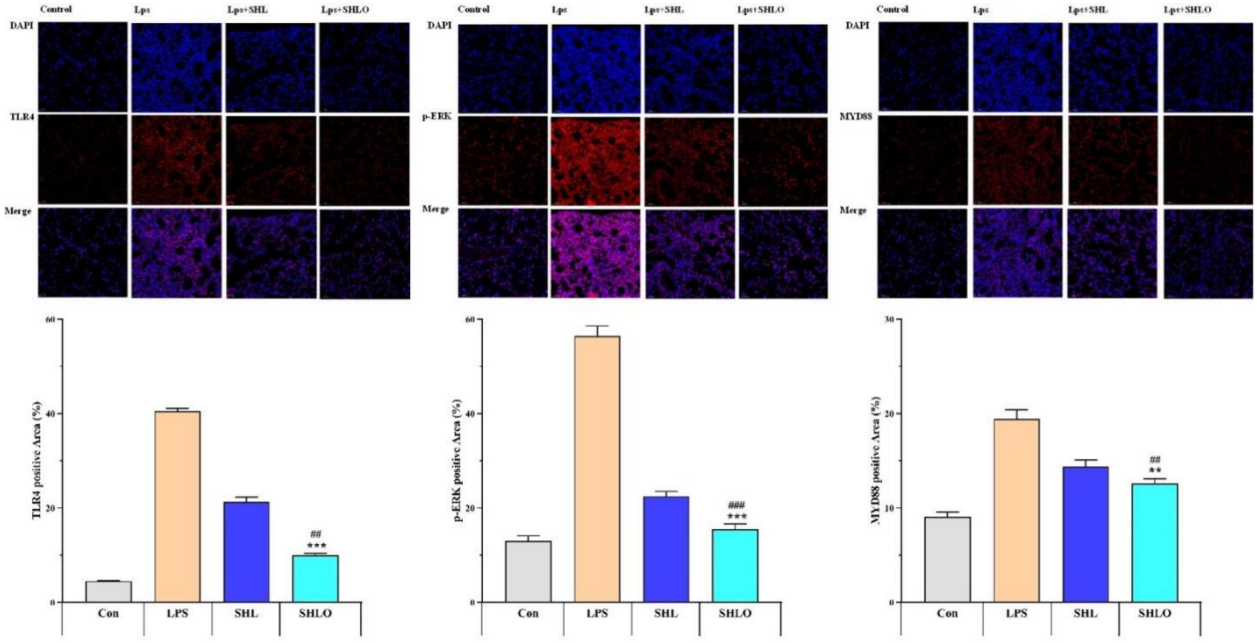

Fig. 6. Immunofluorescence of TLR4, Myd88, and p-ERK in lung tissues. **P<0.01; ***P<0. 001 between LPS and SHLO. ##P<0.05 between SHL and SHLO. Data are described as the mean ± SEM.

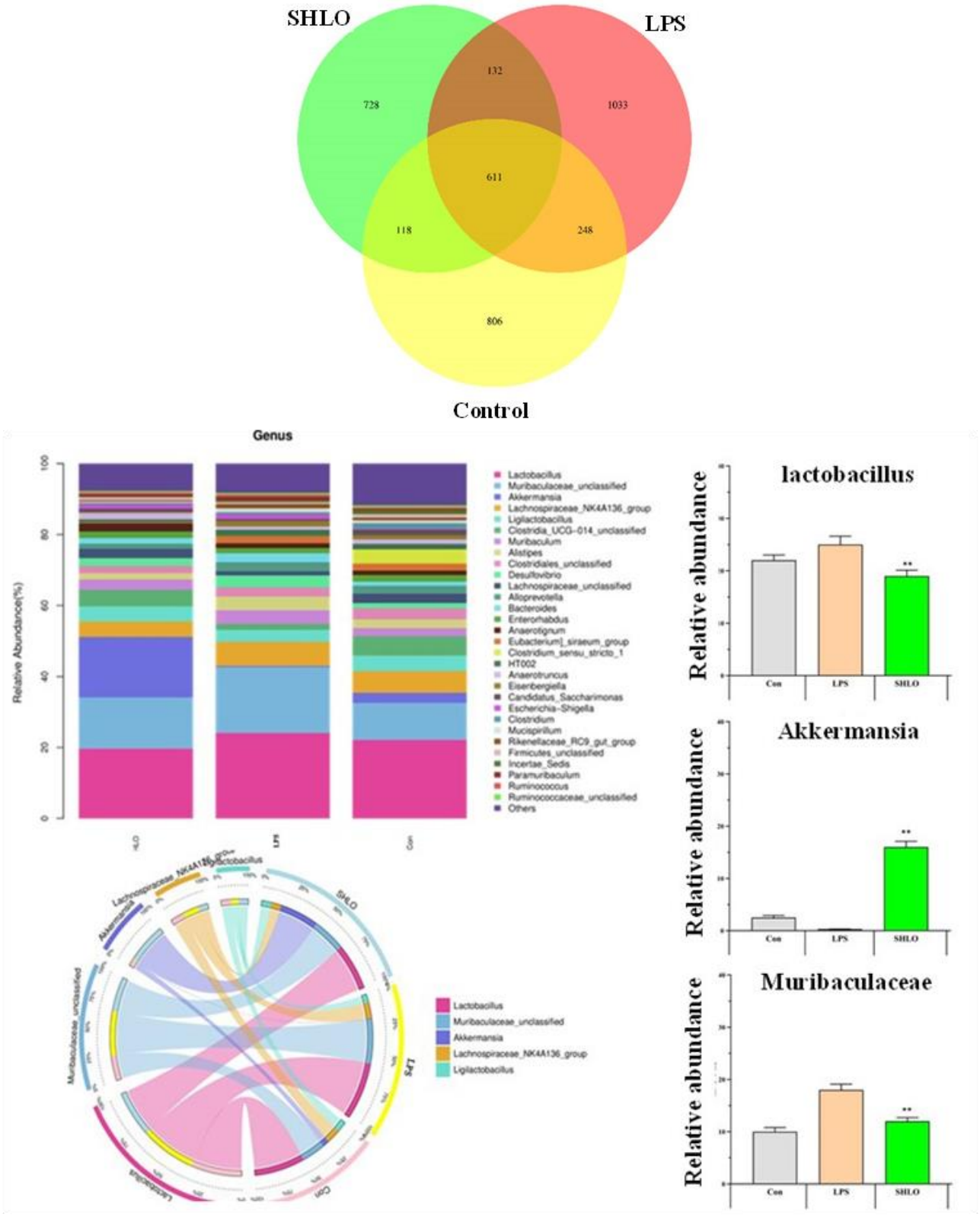

Fig. 7: Effects of LPS and SHLO on the microbial community composition. Venn map showing OTUs and shared OTUs. Relative abundance of microbiota is shown at the genus level. ***P*<0.01 relative abundance between LPS and SHLO.

of inflammation cells, and cascade amplification in the response of inflammation.

TLRs serve as major epithelial receptors for pathogen-associated molecular patterns (PAMPs). Upon activation by LPS, TLR4 triggers the phosphorylation of IκB, a component of the NF-κB complex, leading to its ubiquitination and subsequent dissociation from the complex, therefore activating NF-κB. This signalling cascade transmits the LPS signal downstream (Fan *et al.*, 2021). Additionally, MAPKs, including ERK, JNK, and p38 MAPK, play crucial roles in signal transduction and the regulation of cytokine release (Johnson and Lapadat, 2002; Hassan *et al.*, 2022). In this study, SHLO significantly inhibited the p-ERK phosphorylation in lung

tissues. Furthermore, immunofluorescence results demonstrated that SHLO reduced the expression of TLR4, Myd88, and p-ERK. These findings reaffirm that SHLO may exert its anti-pneumonia effect by modulating the TLR4/Myd88-ERK pathway (Kim *et al.*, 2023). Based on the results of microbial community analysis, the relative abundance of certain (microorganism**)** was significantly increased by LPS-induced acute pneumonia, while SHO decreased their abundance (Morton *et al.*, 2019). Conversely, some microbial reduced by LPS-induced acute pneumonia were elevated by SHLO (Skrzypczak-Wiercioch *et al.*, 2022). These findings collectively support the hypothesis that the gut microbial community plays a decisive role in SHLO's treatment of pneumonia in animals.

Conclusions: In conclusion, SHLO alleviates lung tissue congestion, edema, inflammatory cell infiltration, and collagen deposition which improves lung tissue morphology, reduces fibrosis, and inhibits the expression of inflammatory genes. It suppresses phosphorylation ERK and downregulates TLR4 and Myd88 expression along with regulating intestinal flora. These results offer a foundation for future investigation of the active ingredient in SHLO for treating bacterial pneumonia.

Authors contributions: YH, ZZ, HY, NZ, CL: Conceptualization, Methodology, Formal analysis, Investigation, Resources, Data curation, Writing-Original draft, Writing-Reviewing and Editing. QJ: Methodology, Formal analysis. XZ: Conceptualization, Methodology, Formal analysis, Investigation, Writing-Reviewing and Editing. AR, AEA, LAA, AIM, SM: Conceptualization, Data curation, Writing-Reviewing and Editing.

Funding: This work was supported by the National Key Research and Development Program during the 14th Five-Year Plan Period (2022YFD1801104).

Acknowledgements: Princess Nourah Bint Abdulrahman University Researchers Supporting Project number (PNURSP2024R457), Princess Nourah Bint Abdulrahman University, Riyadh, Saudi Arabia. The authors extend their appreciation to the deanship of scientific research at King Khalid University for supporting this work under the large research group number (R.G.P2/326/45).

REFERENCES

Akpinar D, Mercan T, Demir H, *et al.,* 2023. Protective effects of thymoquinone on doxorubicin-induced lipid peroxidation and antioxidant enzyme levels in rat peripheral tissues. Pak Vet J 43(4):651-658.

Arbaga A, Hassan H, Anis A, *et al*., 2023. Clinicopathological and electrophoretic pattern of serum protein alterations in acute pneumonic sheep. Pak Vet J 43(2):303-308.

Botelho J, Grosso F, Peixe L, *et al*., 2019. Antibiotic resistance in Pseudomonas aeruginosa -mechanisms, epidemiology and evolution. Drug Resist Updates 44:100640.

Chinese Pharmacopoeia Commission, 2017. People's Republic of China Pharmacopoeia Clinical Medication Instructions: Traditional Chinese Medicine Prescription Preparation, vol. 45. Chinese Medicine Science and technology Publishing house, Beijing.

Deshpande R and Zou C, 2020. Pseudomonas aeruginosa induced cell death in acute lung injury and acute respiratory distress syndrome. Int J Mol Sci 21(15):5356.

Ding X, Fan LL, Zhang SX, *et al*., 2022. Traditional chinese medicine in treatment of COVID-19 and viral disease: Efficacies and clinical evidence. Int J Gen Med 15:8353–8363.

Ehrentraut H, Weisheit CK, Frede S, *et al*., 2019. Inducing acute lung injury in mice by direct intratracheal lipopolysaccharide instillation. J Vis Exp 149

Fan YY, Wang J, Feng ZH, *et al.,* 2021. Pinitol attenuates LPS induced pneumonia in experimental animals: Possible role via inhibition of the TLR-4 and NF-κB/IκBα signaling cascade pathway. J of Bio and Mol Toxic, 35(1): e22622.

Gajewski A, Kosmider A, Nowacka A, *et al.,* 2021. Potential of herbal products in prevention and treatment of COVID-19. Literature review. Biomed & Pharm 143:112150.

Hassan F, Aslam B, Muhammad F, *et al.,* 2022. Hypoglycemic properties of Sphaeranthus indicus and Nigella sativa in alloxan-induced diabetes mellitus in rats; a new therapeutic horizon. Pak Vet J 42(2):141-146.

He Y, Xu G, Jiang P, *et al.,* 2023. Antibacterial diarrhea effect and action mechanism of Portulaca oleracea L. water extract based on the regulation of gut microbiota and fecal metabolism. J Sci Food Agric 103(14):7260-7272.

Johnson GL and Lapadat R, 2002. Mitogen-activated protein kinase pathways mediated by ERK, JNK, and p38 protein kinases. Sci 298:1911–1912.

Kim HJ, Kim H, Lee JH, *et al*., 2023. Hwangbo C. Toll-like receptor 4 (TLR4): new insight immune and aging. Immun Ageing 20(1):67.

Lee DYW, Li QY, Liu J. *et al.,* 2021. Traditional Chinese herbal medicine at the forefront battle against COVID-19: clinical experience and scientific basis. Phytomed 80:153337.

Li J, Qin Y, Chen Y, *et al*., 2020. Mechanisms of the lipopolysaccharide-induced inflammatory response in alveolar epithelial cell/macrophage co-culture. Exp Ther Med 20(5):76.

Li L, Wang M, Chen J, *et al.,* 2023. Therapeutic potential of traditional Chinese medicine on heat stroke. Front Pharmacol 14:1228943.

Liu T, Wang HD, Di LQ. *et al.,* 2015. HPLC specific chromatogram spectrum-effect relationship for Shuanghuanglian on MDCK cell injury induced by influenza A virus (H1N1). China J Chinese Mat Med 40(21):4194-4199.

Ma LL, Liu HM, Luo CH, *et al*., 2021. Fever and Antipyretic Supported by Traditional Chinese Medicine: A Multi-Pathway Regulation. Front Pharmacol 12:583279.

Ma Y, Chen M, Guo Y, *et al.,* 2019. Prevention and treatment of infectious diseases by traditional Chinese medicine: a commentary. APMIS 127:372–384.

Men TT, Yen NDH, Kim Tu LT, *et al.,* 2022. Phytochemical constituents and antioxidant activity of some medicinal plants collected from the Mekong Delta, Vietnam. Asian J Agric Biol 2022(4):202105230.

Merad M and Martin JC, 2020. Pathological inflammation in patients with COVID-19: A key role for monocytes and macrophages. Nature Rev Immun 20(6):355-362.

Morton JT, Marotz C, Washburne A, *et al*., 2019. Establishing microbial composition measurement standards with reference frames. Nat Commun 10:2719.

Pang Z, Raudonis R, Glick BR. *et al.,* 2019. Antibiotic resistance in Pseudomonas aeruginosa: mechanisms and alternative therapeutic strategies. Biotechnol Adv 37:177–192.

Quinton LJ, Walkey AJ, Mizgerd JP, *et al.,* 2018. Integrative physiology of pneumonia. Physiol Rev 98(3):1417–1464.

Shi Q, Si D, Bao H, *et al.,* 2019. Efficacy and safety of Chinese medicines for asthma: A systematic review protocol. Medicine (Baltimore) 98(34):e16958.

Shin J, Noh JR, Choe D, *et al., 2022.* Comprehensive 16S rRNA and metagenomic data from the gut microbiome of aging and rejuvenation mouse models. Sci Data 9:197.

Skrzypczak-Wiercioch A and Sałat K, 2022. Lipopolysaccharide-Induced Model of Neuroinflammation: Mechanisms of Action, Research Application and Future Directions for Its Use. Molecules 227(17):5481.

Sun C, Xu Y, Xu G, *et al.,* 2024. Active fractions from Jingfang Baidu Powder alleviate Klebsiella-induced Pneumonia by inhibiting TLR4/Myd88-ERK signaling pathway. J Ethnopharmacol 330:118067

Tang Y, Wang Z, Huo C, *et al*., 2018. Antiviral effects of Shuanghuanglian injection powder against influenza A virus H5N1 in vitro and in vivo. Microb Pathog 121:318-324.

Tsikis ST, Fligor SC, Hirsch TI, *et al*., 2022. Lipopolysaccharide-induced murine lung injury results in long-term pulmonary changes and downregulation of angiogenic pathways. Sci Rep 12:10245.

Vemula S, Mylaram J, Yadala R, *et al.,* 2024. Protective effects of naringenin on 5-fluorouracil induced pulmonary toxicity via modulation of NF-κB and Nrf2 pathway. Pak Vet J 44(1):63-70.

Verjans, E., Kanzler, S., Ohl, K, *et al., 2018.* Initiation of LPS-induced pulmonary dysfunction and its recovery occur independent of T cells. BMC Pulm Med 18:174.

Voiriot G, Dorgham K, Bachelot G, *et al., 2022.* Identification of bronchoalveolar and blood immune-inflammatory biomarker signature associated with poor 28-day outcome in critically ill COVID-19 patients. Sci Rep 12:9502

Wang J, Jiang MM, Chen X, *et al.,* 2020. Cytokine storm and leukocyte changes in mild versus severe SARS-CoV-2 infection: Review of 3939 COVID-19 patients in China and emerging pathogenesis and therapy concepts. J Leukoc Biol 108(1):17-41.

White NM, Balasubramaniam T, Nayak R, *et al.,* 2022. An observational analysis of the trope "A p-value of < 0.05 was considered statistically significant" and other cut-and-paste statistical methods. PLoS One 17(3):e0264360.

Wu CL, Yang ZQ, Hou W, *et al.,* 2005. Experimental study on Shuang huang lian oral liquid againstrespiroviruses (Chin). J Mathem Med 18(6):592-594.

Xi S, Li Y, Yue L, *et al.,* 2020. Role of Traditional Chinese Medicine in the Management of Viral Pneumonia. Front Pharmacol 11:582322.

Yi B, 2018. Therapeutic efficacy of Shuanghuanglian oral liquid (children's type) combined with montelukast in the treatment of pediatric rotavirus enteritis. Chinese J Drug Eval 35(1):48-50.